# Searching for Local Pareto Optimal Solutions: A Case Study on Polygon-Based Problems

Yiping Liu[1], Hisao Ishibuchi[2], Yusuke Nojima[1], Naoki Masuyama[1], and Yuyan Han[3]
[1]Department of Computer Science and Intelligent Systems,
Osaka Prefecture University, Sakai, Osaka 599-8531, Japan
[2]Shenzhen Key Laboratory of Computational Intelligence,
University Key Laboratory of Evolving Intelligent Systems of Guangdong Province,
Department of Computer Science and Engineering,
Southern University of Science and Technology, Shenzhen 518055, China
[3]School of Computer Science, Liaocheng University, Liaocheng, 252059, China
Email: yiping0liu@gmail.com, hisao@sustc.edu.cn, nojima@cs.osakafu-u.ac.jp,
masuyama@cs.osakafu-u.ac.jp, hanyuyan@lcu-cs.com

***Abstract*—Local Pareto optimal solutions may exist in multi-modal multi-objective optimization problems. Traditional multi-objective evolutionary algorithms usually try to escape from local Pareto optima. However, these solutions may be good enough for the decision makers and are additional options if Pareto optimal solutions are infeasible. In this paper, we modify our previous double-niched evolutionary algorithm (DNEA) to search for local Pareto optimal solutions. The new version is termed as DNEA-L. We apply DNEA-L to 3- and 4-objective polygon-based problems with local Pareto optima. The experimental results show that DNEA-L is efficient to find a large number of local Pareto optimal solutions with good diversity.**

***Index Terms*—multi-modal multi-objective optimization, local Pareto optimal solution, niche**

## I. Introduction

Multi-objective optimization problems (MOPs) are commonly seen in real-world applications, such as job shop scheduling [1] and financial portfolio management [2]. Without loss of generality, an MOP can be formulated as follows:

$$\begin{aligned} &\min \boldsymbol{f}(\boldsymbol{x}) = \min(f_1(\boldsymbol{x}), \ldots, f_M(\boldsymbol{x})), \\ &\text{s.t. } \boldsymbol{x} \in S \subset \boldsymbol{R}^n, \end{aligned} \tag{1}$$

where $\boldsymbol{x}$ is an $n$-dimensional decision vector in the decision space $S$, $f_m(\boldsymbol{x})$ is the $m$-th objective to be minimized ($m = 1, ..., M$), and $M$ is the number of objectives. Since these objectives usually conflict with each other, the MOP in (1) has no single optimal solution. Instead, it has a number of Pareto optimal solutions, which are defined as follows:

**Definition 1.** *If there exists no solution in the decision space that dominates $\boldsymbol{x}^*$, then $\boldsymbol{x}^*$ is a Pareto optimal solution.*

This work was supported by National Natural Science Foundation of China (Grant No. 61876075 and 61803192), the Program for Guangdong Introducing Innovative and Enterpreneurial Teams (Grant No. 2017ZT07X386), Shenzhen Peacock Plan (Grant No. KQTD2016112514355531), the Science and Technology Innovation Committee Foundation of Shenzhen (Grant No. ZDSYS201703031748284), and the Program for University Key Laboratory of Guangdong Province (Grant No. 2017KSYS008).

*Corresponding Author: Hisao Ishibuchi*

$\boldsymbol{x}^*$ is also known as a global Pareto optimal solution, since it is non-dominated in the entire decision space. The image of the set of all global Pareto optimal solutions in the objective space is called the Pareto front (PF).

On the other hand, a local Pareto optimal solution [3] is defined as follows:

**Definition 2.** *For a small positive value $\epsilon$, the neighborhood of $\boldsymbol{x}'$ is defined by the set of all solutions within the distance $\epsilon$ from $\boldsymbol{x}'$ in the decision space. If there exists no solution in the neighborhood of $\boldsymbol{x}'$ that dominates $\boldsymbol{x}'$, $\boldsymbol{x}'$ is a local Pareto optimal solution.*

Note that here we do not regard a global Pareto optimal solution as a local one.

If the MOP in (1) has at least one local Pareto optimal solution or at least two different global Pareto optimal solutions for any point on the PF, it is regarded as a multi-modal multi-objective optimization problem (MMOP) [4].

A large number of multi-objective evolutionary algorithms (MOEAs) have been proposed and successfully applied to MOPs over the past two decades, e.g., non-dominated sorting genetic algorithm II (NSGA-II) [5] and MOEA based on decomposition (MOEA/D) [6]. However, they usually cannot handle MMOPs. That is, they are unable to find different global Pareto optimal solutions with the same objective values due to lack of diversity maintenance mechanism in the decision space. They also cannot find local Pareto optimal solutions, since they are designed to escape from local Pareto optimal regions. In traditional multi-objective optimization, only global Pareto optimal solutions are assumed to be useful for the decision maker.

Recently, some multi-modal MOEAs have been proposed to search for different global Pareto optimal solutions with the same objective values, such as Omni-optimizer [7], Niching-CMA [8], decision space based niching NSGA-II (DN-NSGA-II) [9], multi-objective particle swarm optimization algorithm using ring topology and special crowding distance

(MO_Ring_PSO_SCD) [10], double-niched evolutionary algorithm (DNEA) [11], MOEA/D with addition and deletion operators (MOEA/D-AD) [12], and multi-modal multi-objective evolutionary algorithm using two-archive and recombination strategies (TriMOEA-TA&R) [4]. These algorithms are developed based on existing MOEAs. Only non-dominated solutions are preferred in the selections. Therefore, searching for local Pareto optimal solutions is not a design goal in these algorithms.

The quality (i.e., objective values) of local Pareto optimal solutions may be good enough for the decision maker in some applications. They may be quite different from the global Pareto optimal solutions in the decision space. If global Pareto optimal solutions are infeasible due to some factors which are not included in the mathematical model in (1), then finding these solutions will give the decision maker more options.

Therefore, our goal in this study is to find good local Pareto optimal solutions. We propose a variant of DNEA, termed DNEA-L, where an extra archive is used to store multiple non-dominated fronts. Global and local Pareto optimal solutions are expected to be found on those fronts. There are two new parameters in DNEA-L. One is the number of non-dominated fronts to store, i.e., $K$. A larger value of $K$ indicates that local Pareto optimal solutions with worse qualities are acceptable. The other is the neighborhood size $\theta_{nb}$, which is similar to $\epsilon$ in Definition 2. For each solution $\boldsymbol{x}$, the solutions whose distances to $\boldsymbol{x}$ in the decision space are smaller than $\theta_{nb}$ are its neighbors. If a solution is dominated by its neighbors, it is not regarded as a local Pareto optimal solution. A larger value of $\theta_{nb}$ suggests a larger difference in the decision space between a solution on a non-dominated front and solutions on another front. However, $\theta_{nb}$ is usually difficult to specify when we do not have preliminary knowledge about the optimization problem. Therefore, in our method, another parameter $N_{ns}$ is required instead. $N_{ns}$ is the number of nearest solutions to be considered. The algorithm automatically determine $\theta_{nb}$ according to $N_{ns}$, which will be described in Subsection II-B. In the experiments, we apply DNEA-L to polygon-based problems [13] to investigate its ability in finding local Pareto optimal solutions.

The remainder of this paper is organized as below. In Section II, DNEA is briefly introduced. Then, the proposed DNEA-L is described in detail. Section III presents the experimental design and results. Section IV concludes the paper and provides future research directions.

## II. Proposed method

### A. Brief Introduction to DNEA

The general framework of DNEA [11] is similar to standard generational evolutionary algorithms, whereas its environmental selection makes it special.

In the environmental selection, when comparing solutions on the $k$th non-dominated front $F_k$, the double-sharing function $f_{DS}$ of every solution is calculated as follows:

$$f_{DS}(\boldsymbol{x}_i) = \sum_{\boldsymbol{x}_j \in F_k} Sh_{\text{obj}}(i,j) + Sh_{\text{dec}}(i,j), \tag{2}$$

where

$$\begin{aligned} Sh_{\text{obj}}(i,j) &= \max\{0, 1 - d_{\text{obj}}(i,j)/\sigma_{\text{obj}}\}, \\ Sh_{\text{dec}}(i,j) &= \max\{0, 1 - d_{\text{dec}}(i,j)/\sigma_{\text{dec}}\}. \end{aligned} \tag{3}$$

In (3), $d_{\text{obj}}(i,j)$ and $\sigma_{\text{obj}}$ are the Euclidean distance between $\boldsymbol{x}_i$ and $\boldsymbol{x}_j$ and the niche radius in the objective space, respectively, and $d_{\text{dec}}(i,j)$ and $\sigma_{\text{dec}}$ have the similar meanings in the decision space. $f_{DS}$ estimates a solution's density both in the objective and decision spaces. By removing solutions with the largest $f_{DS}$ values, DNEA can maintain a good diversity both in the objective and decision spaces. The experimental results demonstrated its effectiveness on finding different global Pareto optimal solutions with the same objective values. Please refer to [11] for more details.

The experimental results in [11] also showed that DNEA obtained more local Pareto optimal solutions than traditional MOEAs in some cases. However, both the number and the quality of local Pareto optimal solutions cannot be controlled. In this study, we propose DNEA-L to search for local Pareto optimal solutions under controlled conditions.

### B. DNEA-L

The general framework of DNEA-L is presented in Algorithm 1, where a multi-front archive ($A_{MF}$) is employed to store multiple non-dominated fronts. In Algorithm 1, a population $P$ is initialized with a predefined size $N$ (line 1). In each generation (lines 3-7), $N$ parents are selected from $A_{MF}$ to generate a new population (lines 4 and 5). Then, $A_{MF}$ is updated (line 6).

**Algorithm 1** General Framework of DNEA-L

**Require:** $P$ (population), $N$ (population size), $A_{MF}$ (multi-front archive), $K$ (number of non-dominated fronts), $N_{ns}$ (number of nearest solutions)

1: $P$ = *Initialize*($P$) ;
2: $A_{MF}$ = *Multi-Front_Archive_Update*($P$, $N$, $K$, $N_{ns}$);
3: **while** the stopping criterion is not met **do**
4: $P'$ = *Mating_selection*($A_{MF}$, $N$);
5: $P$ = *Reproduction*($P'$);
6: $A_{MF}$ =*Multi-Front_Archive_Update*($P \cup A_{MF}$, $N$, $K$, $N_{ns}$);
7: **end while**
8: **return** $A_{MF}$.

The proposed multi-front archive update method is shown as Algorithm 2. In Algorithm 2, we first calculate the distances between each solution in the candidate solution set $Q$ and its $N_{ns}$ nearest solutions in the decision space. The average distance over $|Q| \times N_{ns}$ distances is used as the neighborhood size $\theta_{nb}$ (line 1). Then, we set $Q' = Q$ (line 2). For each solution $\boldsymbol{x}$ in $Q$, solutions in $Q'$ whose distances to $\boldsymbol{x}$ are smaller than $\theta_{nb}$ in the decision space are defined as the neighbors of $\boldsymbol{x}$ (lines 3-4). All solutions in $Q$ dominated by their neighbors are removed (lines 5-7) since they are not local Pareto optimal solutions. Next, $Q$ is sorted into non-dominated fronts, which are denoted as $F_1 \cup \cdots \cup F_K \cup \ldots$ (line

9). The number of solutions on each of the first $K$ fronts is decreased to $N$ by removing solutions with the largest double-sharing function values in (2) if it is larger than $N$ (lines 11-14). Finally, the first $K$ fronts are united as $A_{MF}$ (line 15). Note that the number of solutions in $A_{MF}$ is not fixed. The maximum size of $A_{MF}$ is $N \times K$.

**Algorithm 2** *Multi-Front_Archive_Update*($Q$, $N$, $K$, $N_{ns}$)

1: Calculate the distances between each solution in $Q$ and its $N_{ns}$ nearest solutions in the decision space. Denote the average distance over $|Q| \times N_{ns}$ distances as $\theta_{nb}$;
2: $Q' = Q$;
3: **for all** $\boldsymbol{x} \in Q$ **do**
4: Find all the solutions in $Q'$ whose distances to $\boldsymbol{x}$ are smaller than $\theta_{nb}$ in the decision space. Denote the set of such solutions as $Q_{nb}$;
5: **if** $\boldsymbol{x}$ is dominated by any solution in $Q_{nb}$ **then**
6: Remove $\boldsymbol{x}$ from $Q$;
7: **end if**
8: **end for**
9: Sort $Q$ into non-dominated fronts, denoted as $F_1 \cup \cdots \cup F_K \cup \ldots$;
10: $A_{MF} = \emptyset$;
11: **for** $k = 1, \ldots, K$ **do**
12: **while** $|F_k| > N$ **do**
13: Remove the solution with the largest double-sharing function value from $F_k$;
14: **end while**
15: $A_{MF} = A_{MF} \cup F_k$;
16: **end for**
17: **return** $A_{MF}$.

Using Algorithm 2, the global and local Pareto optimal solutions with good diversity are expected to be found on the first and the other non-dominated fronts, respectively.

## III. Experiments

### A. Polygon-Based Problems with local Pareto optima

In [11], we proposed polygon-based problems with local Pareto optima, where $I$ equilateral polygons with $M$ vertexes locate in the 2-D decision space. The $m$th vertexes of the $i$th polygon is denoted as $X_{m,i}$, $m = 1, \ldots, M, i = 1, \ldots, I$. The $m$th objective function is

$$f_m(\boldsymbol{x}) = \min\{||\boldsymbol{x} - X_{m,i}||^2,\ i = 1, \ldots, I\}. \quad (4)$$

When the sizes of polygons are different, only the smallest polygon is the global Pareto optimal region, while the others are local Pareto optimal regions.

In this study, the feasible region is $x_1, x_2 \in [-100, 100]$. The center and the distance between a vertex and the center of the first, second, third, and fourth polygons are $(-50, -50)$ and 16, $(50, -50)$ and 20, $(50, 50)$ and 24, and $(-50, 50)$ and 28, respectively.

In Fig. 1, we show 40401 ($201 \times 201$) uniformly sampled solutions in different colors based on their Pareto ranks for the 3- and 4-objective polygon-based problems with local Pareto optima. A brighter (warmer) tone corresponds to a lower Pareto rank. We can see from Fig. 1 that the first polygon is the brightest region. The second, third, and fourth polygons are darker in sequence. It is interesting to note that the vertexes in the second, third, and fourth polygons are brighter than their neighborhood. That is, the solutions close to these vertexes have a lower Pareto rank than their neighbors. These solutions are dominance resistant solutions (DRSs) [14]. One objective value of a DRS is very small, while the others are very large. This makes a DRS having a low chance to be dominated by other solutions.

We can also observe from Fig. 1 that some solutions between two polygons are not darker than their neighbors. This indicates that these solutions could be local Pareto optimal solutions.

To intuitively understand which solutions are global and local Pareto optimal solutions, we first uniformly sample 10201 ($101 \times 101$) solutions in the entire decision space. Then, we remove solutions dominated by their neighbors by setting $\theta_{nb} = 6$. Under this setting, each solution has 24 neighbors. Finally, the remaining solutions are sorted into non-dominated fronts and shown in Fig. 2. Note that in Figs. 2-4, and 6, $\circ$, $\Diamond$, $\triangledown$, $\square$, $\times$, and $*$ denote the solutions on the first, second, third, fourth, fifth, and sixth non-dominated fronts, respectively. $\bullet$ denotes the other local non-dominated solutions. Also, note that setting $\theta_{nb}$ to other values leads to different results. A large value of $\theta_{nb}$ may reduce the number of solutions on each front and the number of fronts. The results under other settings of $\theta_{nb}$ are not provided due to the page limitation.

We can see from Fig. 2 that most solutions on the first four non-dominated fronts locate in the four polygons in sequence. The solutions on the other non-dominated fronts locate between the polygons. It is interesting to note that some solutions on the first four non-dominated fronts are outside the polygons. They are actually not global or local Pareto optimal solutions. The reason is that it is difficult to find solutions that dominate these solutions with a limited number of samples. In the experiments, we use the solutions in Fig. 2 as a reference to observe the behavior of DNEA-L.

### B. Results

In this subsection, we apply DNEA-L and DNEA to the 3- and 4-objective polygon-based problems with local Pareto optima. In both DNEA-L and DNEA, $\sigma_{\text{obj}}$ and $\sigma_{\text{dec}}$ are automatically determined by the average distances between solutions in the objective and decision space, respectively. Simulated binary crossover and polynomial mutation are applied as the crossover and mutation operators, respectively, where the distribution indexes in both operators are set to 20. The crossover and mutation probabilities are 1.0 and 0.5, respectively. The population size is set to 100. The termination criterion of each algorithm is the total number of generations 200. Each algorithm is executed 20 independent runs on each problem.

In the following, we examine the behavior of DNEA-L under different settings of $K$ and $N_{ns}$, respectively.

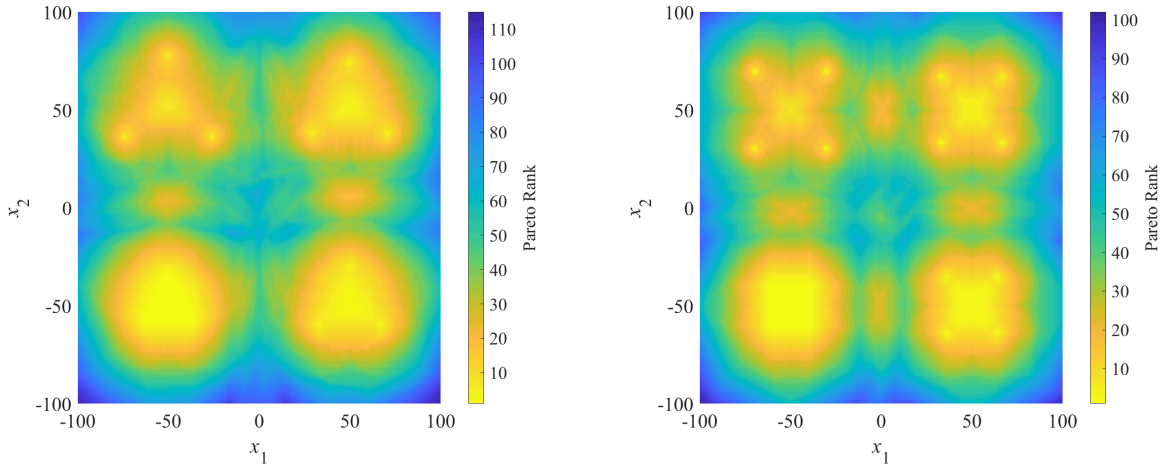


(a) 3-Objective (b) 4-Objective

Fig. 1. 40401 ($201 \times 201$) uniformly sampled solutions in different colors based on their Pareto ranks for 3- and 4-objective polygon-based problems with local Pareto optima. A brighter (warmer) tone corresponds to a lower Pareto rank.

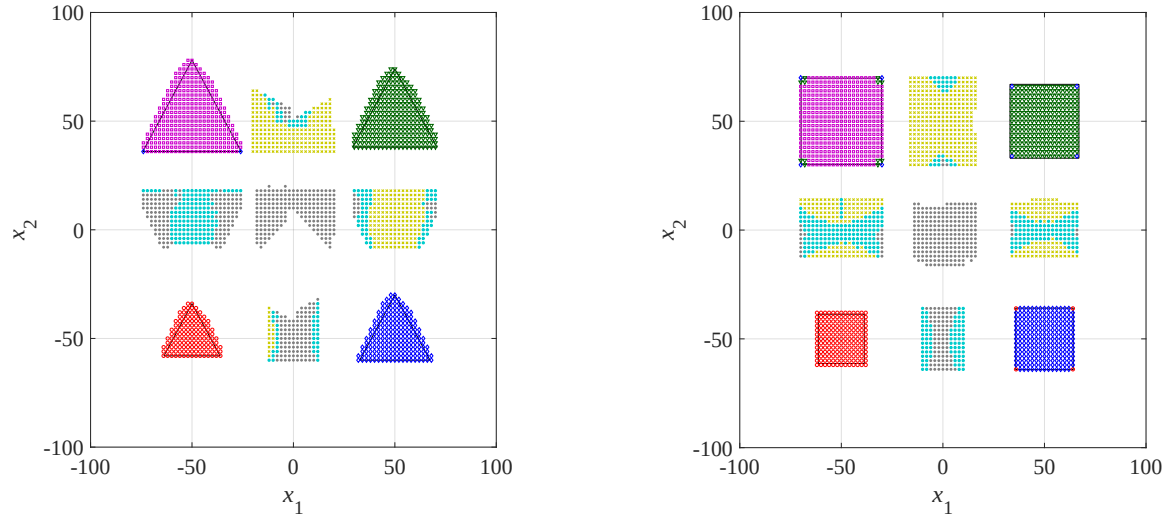


(a) 3-Objective (b) 4-Objective

Fig. 2. The reference global and local non-dominated solutions to the 3- and 4-objective polygon-based problems with local Pareto optima. Note that in Figs. 2-4, and 6, ○, ◊, ▽, □, ×, and ∗ denote the solutions on the first, second, third, fourth, fifth, and sixth non-domiated fronts, respectively. • denotes the other local non-dominated solutions.

*1) Different Settings of $K$:* Table I presents the average hypervolume (HV) obtained by DNEA and DNEA-L with $K = 1$, 2, 3, 4, 5, and 6, respectively (while $N_{ns}$ is set to 25). We also show the hypervolume of the reference solutions in Fig. 2. $\text{HV}_k, k = 1, \ldots, 6$ denotes the HV value of the $k$th non-dominated front. The best (largest) value is in bold face. Note that the maximum value of each objective of the first six non-dominated fronts is around 60. Therefore, we use $(66, \ldots, 66)$ as the reference point to calculate HV. Then we normalize HV into [0,1]. For a more sophisticated reference point specification method, see [15].

In Figs. 3 and 4, we show the solutions obtained by DNEA-L in a single run under different settings of $K$, respectively. This particular run is associated with the result which is the closest to the average $\sum_{k=1,\ldots,6} \text{HV}_k$ in Table I. Since the solutions obtained by DNEA look very similar to those of DNEA-L with $K = 1$, we do not show them due to the page limitation.

We can see from Table I that, no surprisingly, $\text{HV}_1$ of the reference solutions in Fig. 2 is the best, since the distribution of these solutions is almost perfect. However, the differences among $\text{HV}_1$ values in Table I are very small. This indicates that DNEA and DNEA-L under different settings of $K$ can find global Pareto optimal solutions with good diversity. We can also observe from Figs. 3 and 4 that a number of solutions are well distributed in the global Pareto optimal region (the

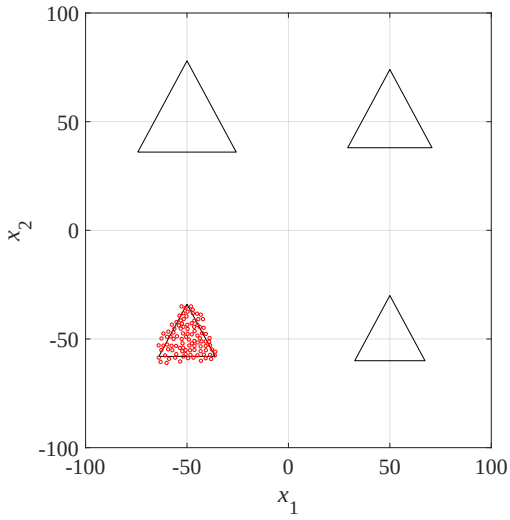


(a) $K = 1$

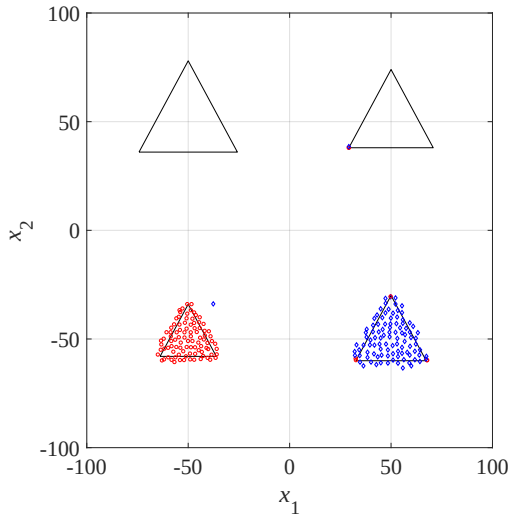


(b) $K = 2$

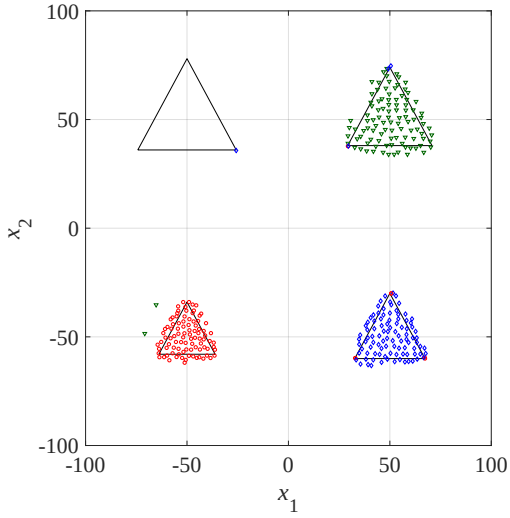


(c) $K = 3$

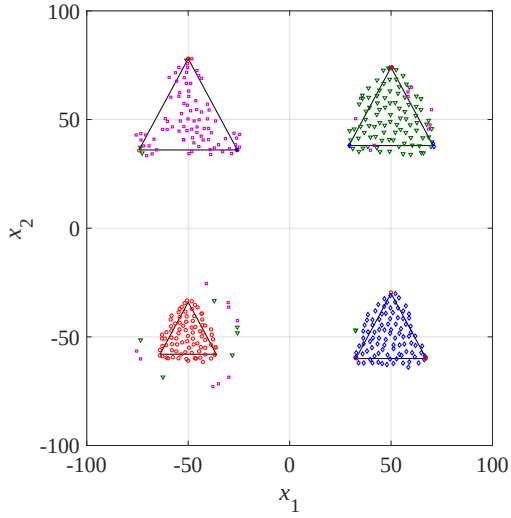


(d) $K = 4$

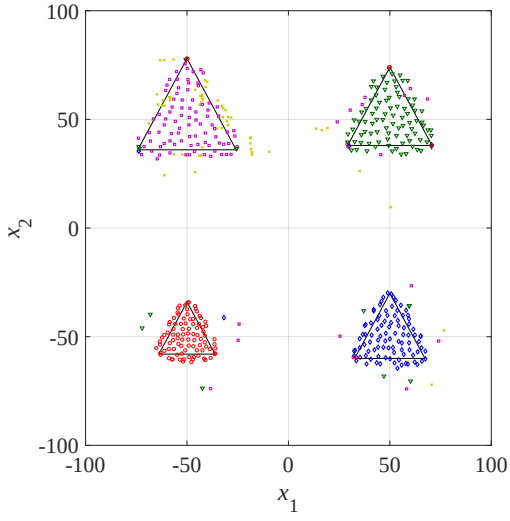


(e) $K = 5$

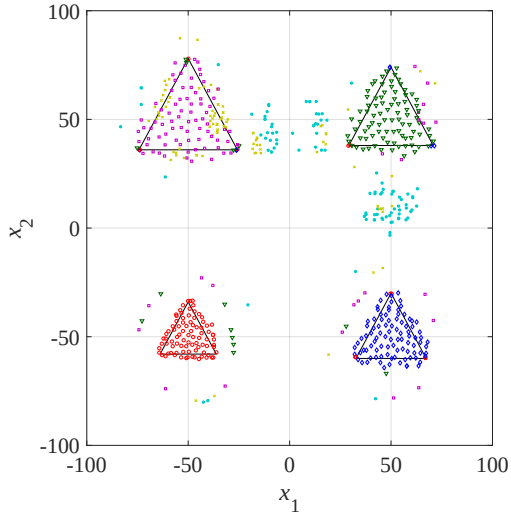


(f) $K = 6$

Fig. 3. The solutions obtained by DNEA-L on the 3-objective polygon-based problem with local Pareto optima under different settings of $K$.

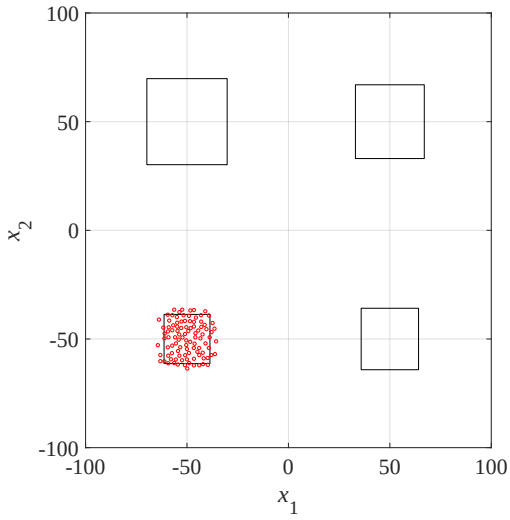


(a) $K = 1$

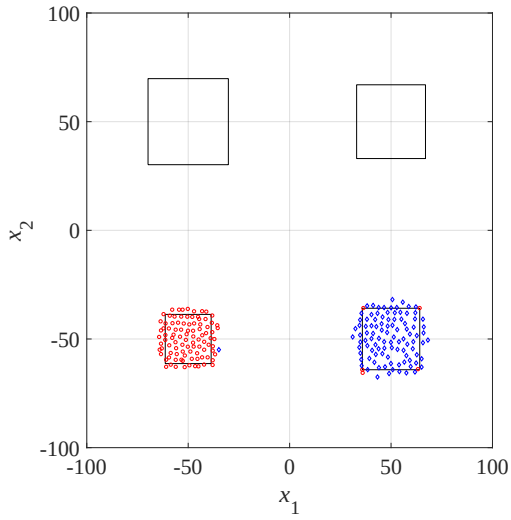


(b) $K = 2$

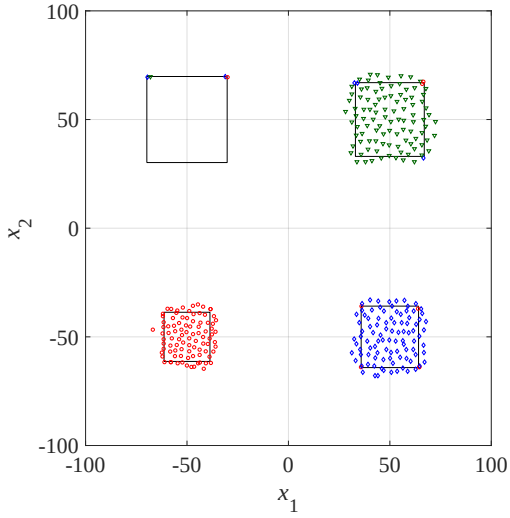


(c) $K = 3$

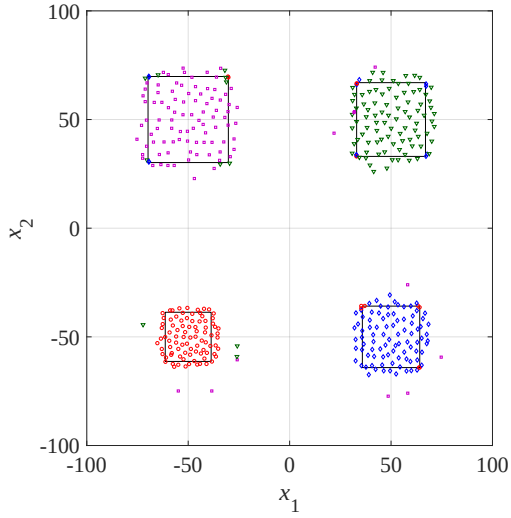


(d) $K = 4$

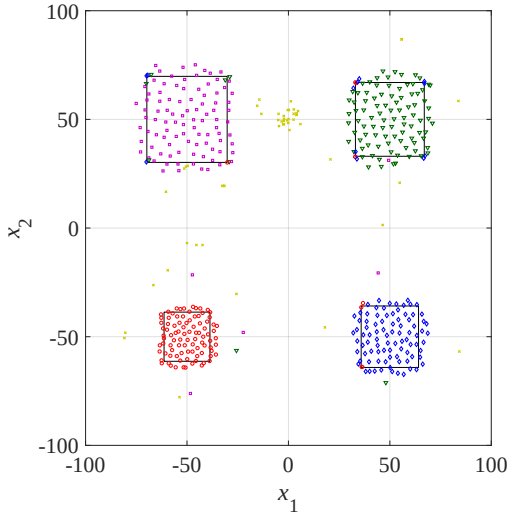


(e) $K = 5$

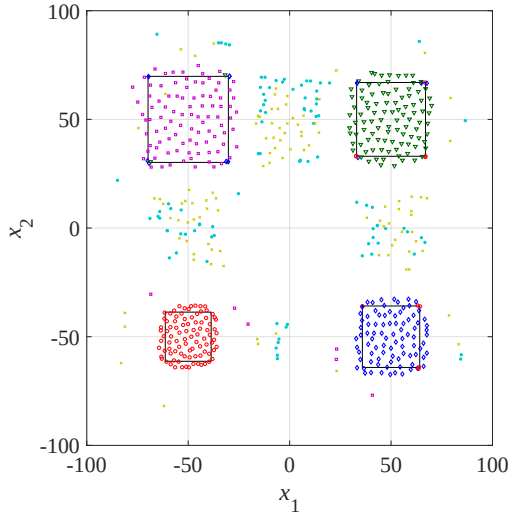


(f) $K = 6$

Fig. 4. The solutions obtained by DNEA-L on the 4-objective polygon-based problem with local Pareto optima under different settings of $K$.

TABLE I
RESULTS OF HYPERVOLUME.

| | | DNEA | DNEA-L ($K$=1) | DNEA-L ($K$=2) | DNEA-L ($K$=3) | DNEA-L ($K$=4) | DNEA-L ($K$=5) | DNEA-L ($K$=6) | Reference in Fig. 2 |
|---|---|---|---|---|---|---|---|---|---|
| 3-Objective | $HV_1$ | 0.7629 | 0.7627 | 0.7714 | 0.7709 | 0.7704 | 0.7706 | 0.7704 | **0.7779** |
| | $HV_2$ | 0.0000 | 0.0000 | 0.6647 | 0.6669 | 0.6677 | 0.6666 | 0.6673 | **0.6779** |
| | $HV_3$ | 0.0000 | 0.0000 | 0.0000 | 0.5611 | 0.5634 | 0.5625 | 0.5622 | **0.5735** |
| | $HV_4$ | 0.0000 | 0.0000 | 0.0000 | 0.0000 | **0.4719** | 0.4712 | 0.4677 | 0.4652 |
| | $HV_5$ | 0.0000 | 0.0000 | 0.0000 | 0.0000 | 0.0000 | 0.3699 | **0.3718** | 0.2654 |
| | $HV_6$ | 0.0000 | 0.0000 | 0.0000 | 0.0000 | 0.0000 | 0.0000 | **0.2714** | 0.1903 |
| 4-Objetive | $HV_1$ | 0.6514 | 0.6497 | 0.6555 | 0.6558 | 0.6544 | 0.6552 | 0.6552 | **0.6625** |
| | $HV_2$ | 0.0000 | 0.0000 | 0.5226 | 0.5255 | 0.5244 | 0.5248 | 0.5246 | **0.5334** |
| | $HV_3$ | 0.0000 | 0.0000 | 0.0000 | 0.4020 | 0.4010 | 0.4011 | 0.4007 | **0.4136** |
| | $HV_4$ | 0.0000 | 0.0000 | 0.0000 | 0.0000 | 0.2935 | 0.2917 | 0.2910 | **0.3049** |
| | $HV_5$ | 0.0000 | 0.0000 | 0.0000 | 0.0000 | 0.0000 | 0.1532 | **0.1536** | 0.1214 |
| | $HV_6$ | 0.0000 | 0.0000 | 0.0000 | 0.0000 | 0.0000 | 0.0000 | **0.0979** | 0.0853 |

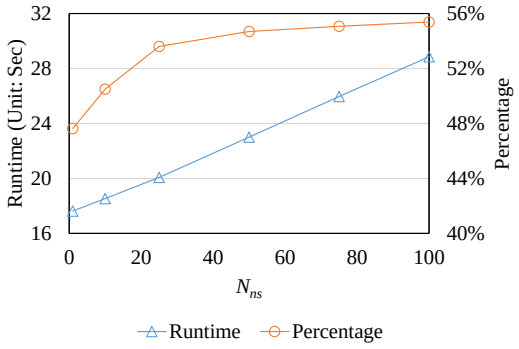


Fig. 5. The average runtimes and the percentages of solutions in the first three polygons when $N_{ns}$ is set to 1, 10, 25, 50, and 100.

left-bottom polygon).

From Table I, the $HV_2, \ldots, HV_K$ values of solutions obtained by DNEA-L are satisfying when $K > 1$. Also, from Figs. 3 and 4, more and more non-dominated fronts are found by DNEA-L by increasing $K$. Most solutions on these non-dominated fronts are local Pareto optimal solutions. The patterns of these solutions are similar to those in Figs. 1 and 2. These observations suggest that DNEA-L is capable of finding local Pareto optimal solutions.

We notice from Table I that when $K > 3$ for the 3-objective problem, $HV_4$, $HV_5$, and/or $HV_6$ obtained by DNEA-L are even better than those of the reference solutions. Similar phenomenon is observed when $K > 4$ for the 4-objective problem. Comparing Figs. 1-4, more solutions which are not local Pareto optimal solutions are obtained by increasing $K$. For example, two solutions on the third non-dominated front are close to the left-bottom triangle in Fig. 3 (c). These solutions are not local Pareto optimal solutions according to Figs. 1 and 2. However, they contribute a lot to the HV value. One reason of obtaining these solutions is that no neighbor solutions dominate these solutions due to a limited archive size (i.e., $K \times N$). Another reason is that $N_{ns}$ is not large enough. Increasing $N$ and/or $N_{ns}$ can reduce the number of such solutions.

*2) Different Settings of $N_{ns}$:* We apply DNEA-L with $N_{ns} = 1, 10, 25, 50, 100$ to the 3-objective problem. Note that $K$ is set to 3. Ideally, all the obtained solutions should locate in the first three polygons. In Fig. 5, we show the average runtimes and the percentages of solutions in the first three polygons under the different settings of $N_{ns}$.

We can see from Fig. 5 that the percentage increases as $N_{ns}$ increases. This indicates that a large value of $N_{ns}$ can reduce the number of the obtained solutions which are neither global nor local Pareto optimal. However, the increase of the percentage is very small when $N_{ns} > 25$. On the other hand, the runtime increases rapidly as $N_{ns}$ increases. Therefore, when the computation resource is limited, we can set $N_{ns}$ to a relatively small value to balance the performance and the computation cost, such as $N_{ns} = 25$ in this case.

In Fig. 6, we show the solutions obtained by DNEA-L in a single run under different settings of $N_{ns}$. From Fig. 6, when $N_{ns} = 1$, a large number of solutions on the second and third non-dominated fronts are obtained outside the first (left-bottom) polygon. These solutions are not local Pareto optimal solutions. As $N_{ns}$ increases, the number of solutions outside the polygons decreases. The results when $N_{ns}$ is set to 75 and 100 look very similar to those when $N_{ns} = 50$. Thus they are not shown here.

## IV. CONCLUSION

In this study, we proposed DNEA-L to search for local Pareto optimal solutions. In DNEA-L, a multi-front archive is used to maintain multiple non-dominated fronts with good diversity both in the objective and decision spaces. The global Pareto optimal solutions are expected to be found on the first non-dominated front, while the local ones are expected to be found on the other fronts.

When using DNEA-L, two parameters should be specified. One is the number of non-dominated fronts to maintain, i.e., $K$. The other is the number of nearest solutions to decide whether a solution is local Pareto optimal, i.e., $N_{ns}$. We applied DNEA-L to 3- and 4-objective polygon-based problems with local Pareto optima under different settings of $K$ and $N_{ns}$. The experimental results show that by increasing $K$, DNEA-L can find more and more local Pareto optimal solutions. Increasing $N_{ns}$ leads to less solutions which are neither global nor local Pareto optimal.

One future work is to apply DNEA-L to other multi-modal multi-objective optimization problems with local Pareto optima. Another is to design a performance metric to evaluate an optimizer's ability in finding local Pareto optima.

## REFERENCES


[1] Y. Han, D. Gong, Y. Jin, and Q. Pan, "Evolutionary multiobjective blocking lot-streaming flow shop scheduling with machine breakdowns," *IEEE transactions on cybernetics*, no. 99, pp. 1–14, 2017.

[2] R. Qi and G. G. Yen, "Hybrid bi-objective portfolio optimization with pre-selection strategy," *Information Sciences*, vol. 417, pp. 401–419, 2017.

[3] Y.-H. Wan, "On local pareto optima," *Journal of Mathematical Economics*, vol. 2, no. 1, pp. 35–42, 1975.

[4] Y. Liu, G. G. Yen, and D. Gong, "A multi-modal multi-objective evolutionary algorithm using two-archive and recombination strategies," *IEEE Transactions on Evolutionary Computation*, 2018. [Online]. Available: http://dx.doi.org/10.1109/TEVC.2018.2879406

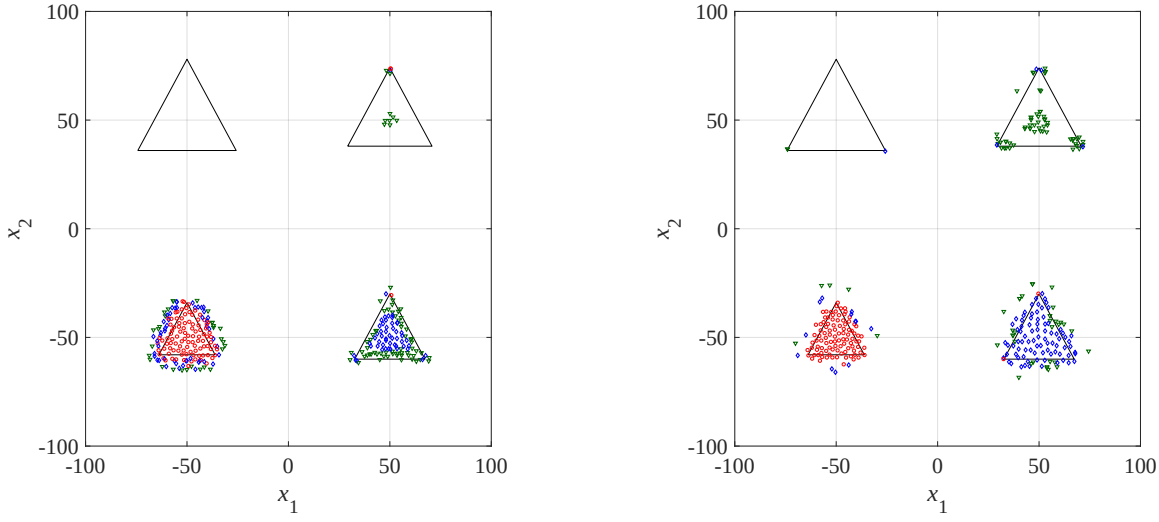


(a) $N_{ns} = 1$ (b) $N_{ns} = 10$

(c) $N_{ns} = 25$ (d) $N_{ns} = 50$

Fig. 6. The solutions obtained by DNEA-L on the 3-objective polygon-based problem with different settings of $N_{ns}$.


[5] K. Deb, A. Pratap, S. Agarwal, and T. Meyarivan, "A fast and elitist multiobjective genetic algorithm: NSGA-II," *IEEE Transactions on Evolutionary Computation*, vol. 6, no. 2, pp. 182–197, 2002.

[6] Q. Zhang and H. Li, "MOEA/D: A multiobjective evolutionary algorithm based on decomposition," *IEEE Transactions on Evolutionary Computation*, vol. 11, no. 6, pp. 712–731, 2007.

[7] K. Deb and S. Tiwari, "Omni-optimizer: A generic evolutionary algorithm for single and multi-objective optimization," *European Journal of Operational Research*, vol. 185, no. 3, pp. 1062–1087, 2008.

[8] O. M. Shir, M. Preuss, B. Naujoks, and M. T. Emmerich, "Enhancing decision space diversity in evolutionary multiobjective algorithms." in *EMO*, vol. 9. Springer, 2009, pp. 95–109.

[9] J. Liang, C. Yue, and B. Qu, "Multimodal multi-objective optimization: A preliminary study," in *2016 IEEE Congress on Evolutionary Computation (CEC)*. IEEE, 2016, pp. 2454–2461.

[10] C. Yue, B. Qu, and J. Liang, "A multiobjective particle swarm optimizer using ring topology for solving multimodal multiobjective problems," *IEEE Transactions on Evolutionary Computation*, vol. 22, no. 5, pp. 805–817, 2018.

[11] Y. Liu, H. Ishibuchi, Y. Nojima, N. Masuyama, and K. Shang, "A double-niched evolutionary algorithm and its behavior on polygon-based problems," in *International Conference on Parallel Problem Solving from Nature*. Springer, 2018, pp. 262–273.

[12] R. Tanabe and H. Ishibuchi, "A decomposition-based evolutionary algorithm for multi-modal multi-objective optimization," in *International Conference on Parallel Problem Solving from Nature*. Springer, 2018, pp. 249–261.

[13] H. Ishibuchi, Y. Hitotsuyanagi, N. Tsukamoto, and Y. Nojima, "Many-objective test problems to visually examine the behavior of multiobjective evolution in a decision space," in *Parallel Problem Solving from Nature, PPSN XI*. Springer, 2010, pp. 91–100.

[14] K. Ikeda, H. Kita, and S. Kobayashi, "Failure of Pareto-based MOEAs: does non-dominated really mean near to optimal?" in *Evolutionary Computation, 2001. Proceedings of the 2001 Congress on*, vol. 2. IEEE, 2001, pp. 957–962.

[15] H. Ishibuchi, R. Imada, Y. Setoguchi, and Y. Nojima, "How to specify a reference point in hypervolume calculation for fair performance comparison," *Evolutionary computation*, vol. 26, no. 3, pp. 411–440, 2018.